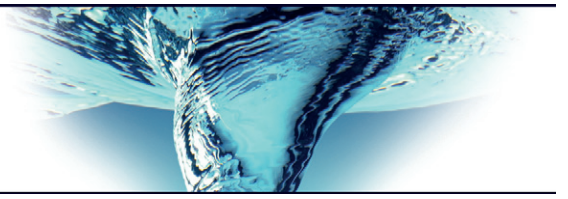
CrossMark

J. Fluid Mech. (2015), *vol.* 767, R4, doi:10.1017/jfm.2015.79



JFM RAPIDS
journals.cambridge.org/rapids

Triadic scale interactions in a turbulent boundary layer

Subrahmanyam Duvvuri[1,†] **and Beverley J. McKeon**[1]

[1]Graduate Aerospace Laboratories, California Institute of Technology, Pasadena, CA 91125, USA

(Received 11 December 2014; revised 26 January 2015; accepted 3 February 2015)

A formal relationship between the skewness and the correlation coefficient of large and small scales, termed the amplitude modulation coefficient, is established for a general statistically stationary signal and is analysed in the context of a turbulent velocity signal. Both the quantities are seen to be measures of phase in triadically consistent interactions between scales of turbulence. The naturally existing phase relationships between large and small scales in a turbulent boundary layer are then manipulated by exciting a synthetic large-scale motion in the flow using a spatially impulsive dynamic wall roughness perturbation. The synthetic scale is seen to alter the phase relationships, or the degree of modulation, in a quasi-deterministic manner by exhibiting a phase-organizing influence on the small scales. The results presented provide encouragement for the development of a practical framework for favourable manipulation of energetic small-scale turbulence through large-scale inputs in a wall-bounded turbulent flow.

Key words: boundary layers, turbulent boundary layers

1. Introduction

The detailed investigation of the bursting phenomenon in a turbulent boundary layer by Rao, Narasimha & Narayanan (1971) provided the first clear evidence of coupling between the large and small scales in the outer and inner regions of the flow respectively. The phase relationship between large and small scales was inferred through scale decomposition and correlation studies by Brown & Thomas (1977) and Bandyopadhyay & Hussain (1984). With advances in experimental and computational techniques, the large- and small-scale relationship in wall-bounded turbulent flows has received considerable attention in more recent times (e.g. see Jacobi & McKeon 2013; Talluru *et al.* 2014, and references therein). An amplitude modulation mechanism was proposed by Hutchins & Marusic (2007), where the amplitude of small scales (high temporal frequencies) is understood as being modulated by the large scales (low temporal frequencies), akin to amplitude modulation of a high-frequency carrier

†Email address for correspondence: subrahmanyam@caltech.edu

© Cambridge University Press 2015

https://doi.org/10.1017/jfm.2015.79 Published online by Cambridge University Press

by a low-frequency signal in radio-wave communication (see Marusic, Mathis & Hutchins 2010). This idea was extended and quantified by Mathis, Hutchins & Marusic (2009) through an elegant demodulation scheme; a correlation coefficient, termed the amplitude modulation coefficient R, between the large-scale streamwise velocity u_L and an envelope of the small-scale velocity u_S was taken to be a measure of amplitude modulation in a turbulent boundary layer. Using a cospectral technique, Jacobi & McKeon (2013) showed that the very-large-scale motions (VLSMs) are the dominant modulating scale in u_L. An interesting similarity in the behaviour of R and the skewness of streamwise velocity fluctuations S with wall-normal distance was also noted by Mathis *et al.* (2009), but was not explored further.

The interpretation of the large- and small-scale correlation as an amplitude modulation was met with caution by Schlatter & Örlu (2010); they suggested that R is to a great extent another representation of the cross-terms of the scale-decomposed skewness. Mathis *et al.* (2011) confirmed the similarity between R and S by showing that the cross-term $3u_L u_S^2$, obtained by a scale decomposition ($u = u_L + u_S$) of S, mimics the behaviour of R with wall-normal height across a range of Reynolds numbers in turbulent boundary layers. Chung & McKeon (2010) noted that R can also be interpreted as a phase relationship between the large scales and the small-scale envelope. It is now clear that, at the very least, a definitive phase relationship exists between large- and small-scale activity due to nonlinear coupling in wall-bounded turbulent flows.

In this paper we first establish a formal relationship between S and R through a simple multiscale analysis of a general statistically stationary signal. It is shown that both S and R can be considered as measures of phase in triadically consistent interactions between scales. The significance of the triadic phase in turbulent flows stems from the fact that the nonlinearity in the governing Navier–Stokes equations is quadratic, and hence the nonlinear coupling between scales is of triadic nature. We then describe and present results from an experiment in which a synthetic spanwise-constant large-scale motion is excited (or forced) in a flat-plate turbulent boundary layer. The synthetic scale results in significant changes in the values of S and R, thereby implying a modified phase relationship between scales. The effects of the synthetic scale are felt strongly by directly coupled small scales through triadic interactions; the synthetic scale is seen to have a clear phase-organizing or phase-locking effect on the triadic small-scale envelope.

2. Triadic scale interactions

2.1. *Skewness*

We begin our analysis by considering a general statistically stationary velocity signal $u(x)$ in the streamwise direction x. The signal is decomposed into its Fourier modes with wavenumbers k_i and corresponding amplitudes and phases α_i and ϕ_i respectively,

$$\begin{aligned} u \;=\; & \alpha_1 \sin(k_1 x + \phi_1) + \alpha_2 \sin(k_2 x + \phi_2) \cdots + \alpha_i \sin(k_i x + \phi_i) \ldots \text{to } k_\infty, \\ & \text{with } 0 < k_1 < k_2 < \cdots < k_i < \cdots < k_\infty. \end{aligned} \tag{2.1}$$

With σ as the standard deviation of u, the skewness S is written as a triple sum

$$\sigma^3 S = \langle u^3 \rangle = \sum_{l=1}^{\infty} \sum_{m=1}^{\infty} \sum_{n=1}^{\infty} \alpha_l \alpha_m \alpha_n \langle \sin(k_l x + \phi_l) \sin(k_m x + \phi_m) \sin(k_n x + \phi_n) \rangle, \tag{2.2}$$

https://doi.org/10.1017/jfm.2015.79 Published online by Cambridge University Press

where $\langle\,\rangle$ denotes the mean operator. The triple sum in the above equation can be manipulated using a simple trigonometric identity, and by the orthogonal nature of sinusoids it can be shown that only triadic combinations of k_l, k_m, k_n with $k_l = k_n - k_m$ and wavenumber pairs k_l, k_n with $k_n = 2k_l$ make non-zero contributions to S. It should be noted that here we assume $k_l < k_m < k_n$ without a loss of generality. The skewness S can then be reduced to the following form:

$$S = \frac{6}{4\sigma^3} \sum_{\substack{\forall l,m,n| \\ k_l<k_m<k_n \\ k_l+k_m=k_n}} \alpha_l\alpha_m\alpha_n \sin(\phi_l + \phi_m - \phi_n) + \frac{3}{4\sigma^3} \sum_{\substack{l=1 \\ k_n=2k_l}}^{\infty} \alpha_l^2\alpha_n \sin(2\phi_l - \phi_n). \tag{2.3}$$

From the above equation it is seen that the skewness is nothing but a weighted (by mode amplitudes) and normalized (by σ^3) sum of the quantity $\sin(\phi_l + \phi_m - \phi_n)$ over all sets of triads and wavenumber pairs. It is shown next by considering R that $\sin(\phi_l + \phi_m - \phi_n)$ is a measure of the phase difference between the mode $\sin(k_l x + \phi_l)$ and the envelope of higher wavenumber modes $\sin(k_m x + \phi_m)$ and $\sin(k_n x + \phi_n)$.

2.2. *Amplitude modulation coefficient*

The procedure to calculate R as outlined by Mathis *et al.* (2009) is followed here, but with a slight departure in the enveloping technique which is explained below. First, the velocity signal u is split into large- and small-scale components using a spatial Fourier filter at a set wavenumber, arbitrarily chosen as k_γ (see figure 1). We then have the large- and small-scale velocity signals u_L and u_S,

$$\left.\begin{aligned} u_L &= \alpha_1 \sin(k_1 x + \phi_1) \cdots + \alpha_l \sin(k_l x + \phi_l) \cdots + \alpha_{\gamma-1} \sin(k_{\gamma-1} x + \phi_{\gamma-1}), \\ u_S &= \alpha_\gamma \sin(k_\gamma x + \phi_\gamma) \cdots + \alpha_m \sin(k_m x + \phi_m) \cdots + \alpha_n \sin(k_n x + \phi_n) \ldots \text{ to } k_\infty. \end{aligned}\right\} \tag{2.4}$$

Here again we assume without a loss of generality that $k_l < k_\gamma < k_m < k_n$. Next, an envelope function $\mathscr{E}(x)$ for the small-scale velocity signal is obtained using the Hilbert transform. Mathis *et al.* (2009) use the analytic signal A, written as $A(x) = \sqrt{u_S^2(x) + \mathscr{H}^2(x)}$, where $\mathscr{H}(x)$ is the Hilbert transform of $u_S(x)$, as an envelope of the small-scale activity. Here we take A^2 to be our envelope function, i.e. $\mathscr{E}(x) = A^2(x)$. This allows for a more direct interpretation of the final result in terms of phase in triadic interactions. For the purposes of forming a correlation coefficient, as in the calculation of R, $A^2(x)$ is a valid proxy for $A(x)$. As R is a normalized measure, no significant differences are expected in its value between the cases of $A(x)$ and $A^2(x)$ being used as the envelope function, and this was easily verified by experimental data (not shown here). Following the rest of the procedure, and with some trigonometric manipulation, the expression for R can be reduced to the form

$$R = \frac{1}{\Omega} \sum_{\substack{\forall l,m,n| \\ k_n-k_m=k_l \\ 0<k_l<k_\gamma \\ k_m,k_n>k_\gamma}} \alpha_l\alpha_m\alpha_n \sin(\phi_l + \phi_m - \phi_n), \tag{2.5}$$

where $\Omega = \sqrt{\langle \mathscr{E}_L^2 \rangle \langle u_L^2 \rangle}$ is the normalization factor for the covariance $\langle \mathscr{E}_L u_L \rangle$, with $\mathscr{E}_L$ denoting the large-scale-pass filtered envelope function. As in the case of S, only triadic interactions between wavenumbers have non-zero contributions to R.

https://doi.org/10.1017/jfm.2015.79 Published online by Cambridge University Press

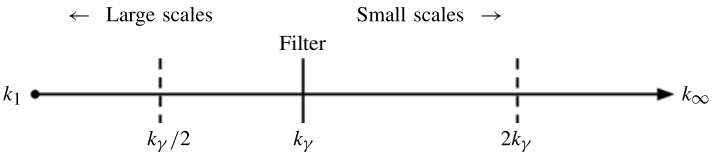


FIGURE 1. A schematic of the wavenumber line.

Following the phase interpretation of Chung & McKeon (2010), it is seen that $\phi_l + \phi_m - \phi_n = \Delta\phi$ in the above equation is the phase difference between the large scale k_l and the envelope of the triadic small scales k_m, k_n. Hence, R can be interpreted as an amplitude-weighted (and normalized) phase measure $\sin(\Delta\phi)$ of all triadic interactions where the large scale and the two triadic small scales fall on either side of the filter cutoff. It should be noticed that the skewness (2.3) is also a measure of the same phase quantity, but over all triadic interactions without any filter restrictions. The similarity between S and R was first pointed out by Sharma & McKeon (2013) for a single triad, i.e. a single set of three triadically consistent wavenumbers. Although S and R exhibit similar trends with wall-normal height in a turbulent boundary layer, it is easy to see from (2.3) and (2.5) that differences exist between the two. This is discussed in the following subsection, and an analytical relationship is established between the two phase measures.

2.3. *An exact relationship between the skewness and the amplitude modulation coefficient*

There are significant differences between measured values of S and R in the near-wall and the outer-wake regions of a turbulent boundary layer (see for instance Mathis *et al.* 2011, figure 1). These differences can be understood by a direct comparison of (2.3) and (2.5); S accounts for triadic and wavenumber pair interactions over the entire wavenumber range, whereas R accounts for only those triadic interactions that occur across the filter cutoff location k_γ (see figure 1). Moreover, the weights and normalization factors for triadic interactions in S and R are different. The triadic and wavenumber pair interactions captured by S but not by R can be accounted for by considering the three quantities $\langle u_S^3\rangle$, $\langle u_L^3\rangle$, $\langle u_L^2 u_S\rangle$, as explained below with reference to the schematic shown in figure 1.

(i) $\langle u_S^3\rangle$: u_S only contains velocity scales with wavenumbers greater than k_γ, hence $\langle u_S^3\rangle$ captures all triadic and wavenumber pair interactions to the right of the filter. This is similar to $\langle u^3\rangle$, but $\langle u^3\rangle$ captures those interactions across the entire wavenumber line whereas $\langle u_S^3\rangle$ is band-limited, and likely to be most active close to the wall.

(ii) $\langle u_L^3\rangle$: u_L only contains velocity scales with wavenumbers smaller than k_γ; hence $\langle u_L^3\rangle$ captures triadic interactions to the left of the filter where the two smaller wavenumbers are less than $k_\gamma/2$, and wavenumber pair interactions for all wavenumbers k_l, k_n such that $k_n = 2k_l$ and $k_1 < k_l < k_\gamma/2$. Larger-scale activity is most prevalent in the wake region.

(iii) $\langle u_L^2 u_S\rangle$: with workings similar to S and R in (2.3) and (2.5) respectively, it can be shown that $\langle u_L^2 u_S\rangle$ reduces to the following form:

$$\langle u_L^2 u_S\rangle = \frac{1}{2} \sum_{\substack{\forall l,m,n| \\ k_l<k_m<k_\gamma<k_n \\ k_\gamma/2<k_m \\ k_l+k_m=k_n}} \alpha_l\alpha_m\alpha_n \sin(\phi_l+\phi_m-\phi_n) + \frac{1}{4} \sum_{\substack{l=\gamma/2 \\ k_n=2k_l}}^{\gamma} \alpha_l^2\alpha_n \sin(2\phi_l-\phi_n). \tag{2.6}$$

https://doi.org/10.1017/jfm.2015.79 Published online by Cambridge University Press

The first term on the right-hand side captures triadic interactions where the intermediate wavenumber necessarily lies in between $k_\gamma/2$ and k_γ, and the second term captures wavenumber pair interactions for all wavenumbers k_l, k_n such that $k_n = 2k_l$ and $k_\gamma/2 < k_l < k_\gamma$.

From the above descriptions of $\langle u_S^3 \rangle$, $\langle u_L^3 \rangle$ and $\langle u_L^2 u_S \rangle$, it is seen that the three quantities exactly capture the triadic and wavenumber interactions accounted for by S and missed by R. An analytical relationship can now be established between S and R. Balancing the weights between S, R, $\langle u_S^3 \rangle$, $\langle u_L^3 \rangle$ and $\langle u_L^2 u_S \rangle$ gives

$$\sigma^3 S = 1.5\Omega R + \langle u_S^3 \rangle + \langle u_L^3 \rangle + 3\langle u_L^2 u_S \rangle. \tag{2.7}$$

The terms on the right-hand side have a clear resemblance to scale-decomposed skewness, but with a scaled version of R replacing $3\langle u_L u_S^2 \rangle$. This confirms the suggestion of Mathis *et al.* (2011) that the cross-term $3\langle u_L u_S^2 \rangle$ can be used as an alternative or complementary diagnostic tool to R.

It is worth noting that the analysis presented thus far makes no assumptions regarding the underlying dynamics of the system that generates the signal u. Hence (2.7) is applicable to any statistically stationary signal in general. This helps in understanding the results of the amplitude modulation coefficient presented by Mathis *et al.* (2009) and Schlatter & Örlu (2010) for synthetic turbulent signals. Mathis *et al.* (2009) show that $R(y)$ is nearly zero when phase information is randomly scrambled in velocity signals obtained from a turbulent boundary layer. By assigning random phases to different scales, we expect that on average the phase difference between large scales and the envelopes of two triadically interacting small scales ($\Delta\phi$) will be zero, and hence $R(y) \approx 0$. Schlatter & Örlu (2010) consider synthetic signals with matched probability density functions (PDFs) to real turbulent signals but with no scale (amplitude) information contained in them. However, by matching the PDF (and hence skewness), they retain the phase information contained in the real signal. Although all amplitude information is removed from the signal, as R is a normalized measure, it is not surprising to see that there is a good match between $R(y)$ calculated from their real and synthetic signals.

It is seen from this analysis that both the skewness and the amplitude modulation coefficient are amplitude-weighted average measures of phase in triadic scale interactions. It should be noted that the extension of this analysis to a broader definition of triadic interactions, for example including the spanwise wavenumber and temporal frequency, is straightforward. In the following section we describe an experiment in which the natural phase relationships between scales in a turbulent boundary layer are altered by exciting a synthetic large-scale motion in the flow.

3. Synthetic large scale in a turbulent boundary layer

3.1. *The experiment*

A zero-pressure-gradient turbulent boundary-layer flow over a smooth flat plate was set up for this study in the Merrill wind tunnel at Caltech. A spanwise-constant spatio-temporal mode was excited (or forced) in the flow following the technique of Jacobi & McKeon (2011) with modifications. Details of the experiment were presented recently by the authors (Duvvuri & McKeon 2014), and are recounted here in brief for the sake of completeness. Detailed description of a similar experiment can also be found in Jacobi & McKeon (2011). Figure 2(*a*) shows a schematic of the flat plate and the roughness perturbation in the form of a thin rib aligned along the spanwise direction.

https://doi.org/10.1017/jfm.2015.79 Published online by Cambridge University Press

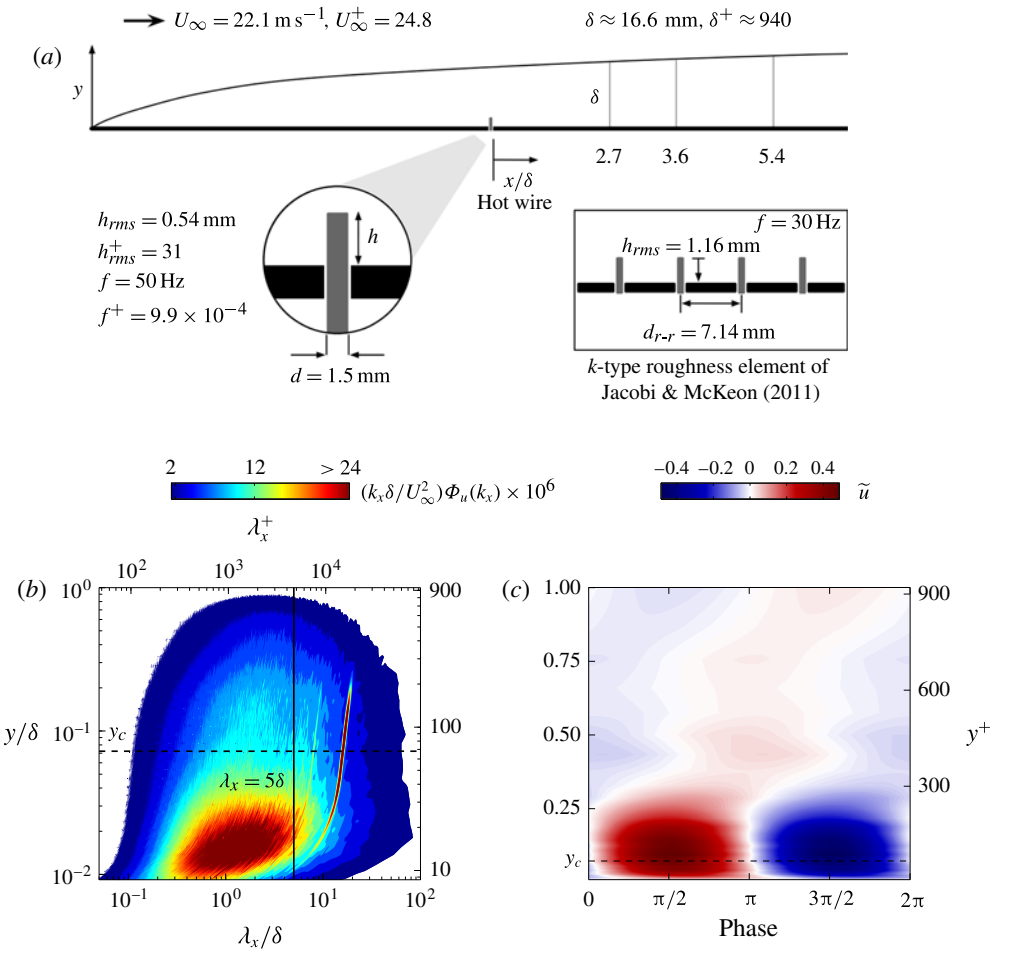


FIGURE 2. Schematic of the experimental set-up (not to scale), spectral data and synthetic mode shape. (*a*) The turbulent boundary layer is forced by a spatially impulsive single rib dynamic roughness, and phase-locked hot-wire measurements are made at three downstream stations as marked. Here, momentum thickness Reynolds number $Re_\theta = 2780$ and friction Reynolds number $Re_\tau = 940$ at the first measurement station $x = 2.7\delta$, where δ is the boundary layer thickness. The *k*-type roughness of Jacobi & McKeon (2011) is shown as an inset at the bottom right of the figure for comparison. (*b*) Premultiplied power spectrum of streamwise velocity fluctuations at $x = 2.7\delta$ (log scale in y). (*c*) Synthetic mode shape over one temporal period $x = 2.7\delta$ (linear scale in y, contour scale in m s^{-1}).

The boundary layer with a free-stream velocity of $U_\infty = 22.1$ m s^{-1} is fully turbulent with $Re_\theta \approx 2750$ at the perturbation rib location. The rib was oscillated sinusoidally at a frequency $f = 50$ Hz in the wall-normal direction y with a peak-to-trough amplitude of $h = 0.76$ mm ($h_{rms} = 0.54 \pm 0.02$ mm) such that the rib sat flush with the plate surface at the trough of every oscillation cycle.

The dynamic roughness perturbation introduces a dominant temporal scale and a dominant streamwise length scale (i.e. a travelling wave or a spatio-temporal mode) in the boundary layer downstream; the temporal scale corresponds to the time period of forcing ($1/f$), and the length scale is a function of the roughness geometry. The *k*-type roughness element used by Jacobi & McKeon (2011) is shown as an inset in

https://doi.org/10.1017/jfm.2015.79 Published online by Cambridge University Press

figure 2 for comparison with the present study. Along with dynamic forcing effects, significant static roughness effects are reported by Jacobi & McKeon (2011). Here, the number of roughness ribs was reduced from four to one, and the perturbation amplitude was decreased from $h_{rms} = 1.16$ to 0.54 mm. With a significantly shorter streamwise extent and reduced mean blockage, any static roughness effects due to the relatively weaker perturbation at the downstream measurement locations were minimal (see the mean velocity profiles in figure 3*a*). Moreover, the oscillation frequency was increased from $f = 30$ to 50 Hz to generate sufficiently strong dynamic forcing effects. It is important to note at this point that multiple scales are excited by static roughness effects immediately downstream of the perturbation ($x < 1\delta$); this is seen in the experimental data of Jacobi & McKeon (2011). However, these evanescent modes decay quickly and the flow is dominated by a single spatio-temporal mode for a relatively large streamwise extent.

Hot-wire measurements were made at three different stations downstream of the roughness in the canonical (no roughness perturbation, fully smooth plate) and dynamically perturbed (or forced) flows using a Dantec 55P05 boundary-layer probe (5 μm diameter and 1.25 mm active length) with a Dantec StreamLine Pro anemometer.

3.2. *Results: statistics, spectrum and synthetic mode shape*

Data from hot-wire measurements made at the first station $x = 2.7\delta$ downstream of the perturbation, herein referred to as station-1, are used for most of the analysis presented here. The boundary-layer thickness δ at station-1 based on 99 % of U_∞ was 16.55 mm, and the momentum-thickness-based Reynolds number Re_θ was 2780 for the canonical flow. The friction Reynolds number Re_τ was estimated to be 940 using the Coles–Fernholz empirical relation, $C_f = 2[\kappa^{-1}\log(Re_\theta) + C]^{-2}$; here C_f is the skin-friction coefficient. The relation was also used to estimate Re_τ for the forced flow, and wall-normal distances and streamwise wavelengths are scaled in inner units along with outer units in figures. It should be noted that the Coles–Fernholz estimate is strictly applicable only to the canonical flow; however, viscous scaling in the figures provides a useful reference. The instantaneous streamwise velocity $U(y, t)$, where t is time, is decomposed into a time mean $\overline{U}(y)$ and a fluctuating component $u(y, t)$ (Reynolds decomposition). Profiles of $\overline{U}(y)$ and variance of $u(y, t)$ at station-1 are shown in figure 3(*a*). The dynamic forcing effect is clearly seen in the form of an energetic bulge in the variance profile of the forced flow; this results from the excitation of a synthetic scale in the flow. As the forcing is spatially impulsive and applied only at one location, the energy associated with the synthetic scale decays with the downstream distance, and eventually the variance profile collapses onto the canonical case (see Duvvuri & McKeon 2014, figure 2). As the mean velocity profiles of the canonical and forced flows almost overlap, there is no significant change in δ and Re_τ between the two flows.

Figure 2(*b*) shows the premultiplied power spectrum of u for the forced flow at station-1 (for the corresponding spectrum of the unforced case, see Duvvuri & McKeon 2014). Taylor's hypothesis of frozen turbulence is used to project temporal velocity fluctuations to the streamwise spatial direction through the local mean velocity. The presence of a synthetic large scale in the forced boundary layer is distinctly seen in the spectrum of the forced flow. In a strict sense, the following analysis is valid only in the temporal domain. However, the energetic content of the synthetic mode is centred sufficiently far from the wall that any errors associated

https://doi.org/10.1017/jfm.2015.79 Published online by Cambridge University Press

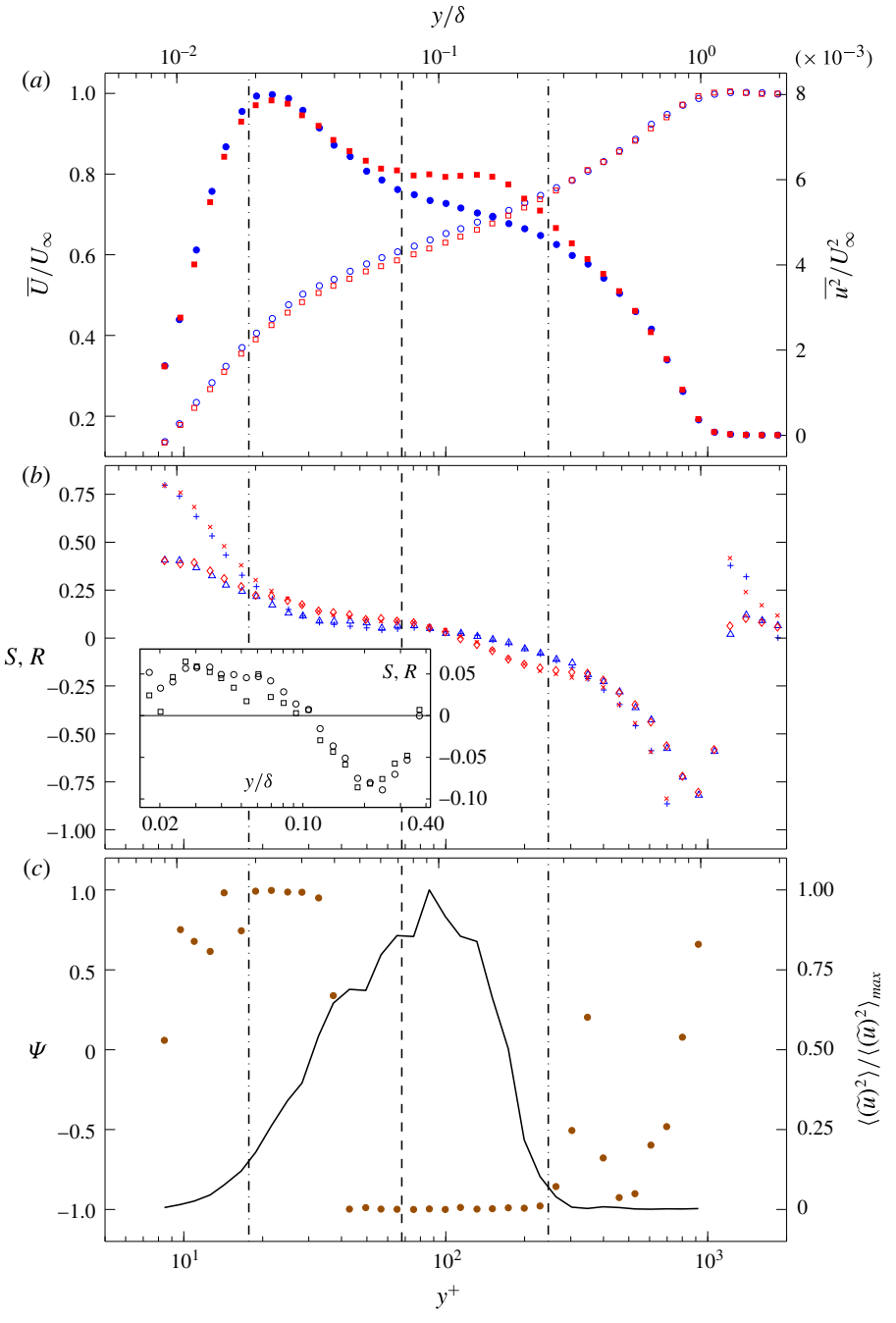


FIGURE 3. Statistical and phase data from station-1. The dashed line is the estimated critical layer location and the dash-dot lines are the locations where the synthetic mode energy drops to 15 % of its maximum value. (*a*) Mean streamwise velocity profiles: canonical flow (CF), ○; forced flow (FF), □. Variance profiles: CF, ●; FF, ■. (*b*) Skewness (*S*): CF, +; FF, ×. Amplitude modulation coefficient (*R*): CF, △; FF, ◇. The inset shows the difference between FF and CF for *S* (○) and *R* (□). (*c*) Correlation coefficient Ψ (●) and normalized synthetic mode energy (–).

https://doi.org/10.1017/jfm.2015.79 Published online by Cambridge University Press

with Taylor's hypothesis are unlikely to be sufficiently large to cause significant contamination of the results, and the conclusions presented here remain unaffected by projection from t to x. There is clear scale separation between the synthetic large scale and the energetic small scales that constitute the near-wall cycle of turbulence. A spatial Fourier filter is used to separate the velocity fluctuations u into large and small scales ($u = u_L + u_S$) for calculation of R. The cutoff for the filter was chosen as $\lambda_\gamma = 2\pi/k_\gamma = 5\delta$ (marked by a vertical line in figure 2*b*), where the separation between the synthetic large scale and the energetic small scales is clear for all y.

Following Hussain & Reynolds (1970), the turbulent fluctuations $u(y, t)$ are further decomposed as $u(y, t) = \widetilde{u}(y) + u'(y, t)$ into coherent and turbulent parts; here, $\widetilde{u}$ is the periodic velocity component associated with the forcing and u' is the rest of the turbulence. The periodic velocity component $\widetilde{u}(y)$ is obtained by subjecting $u(y, t)$ to a narrow-band-pass filter around the forcing frequency and then phase averaging the filter output with respect to the input forcing signal (for details, see Duvvuri & McKeon 2014); it represents the amplitude and shape of the synthetic mode. Figure 2(*c*) shows $\widetilde{u}(y)$ at station-1 ($x = 2.7\delta$) over one temporal period. The periodic velocity component $\widetilde{u}(y)$ is also calculated at $x = 3.6\delta$ and $x = 5.4\delta$ (not shown here); by tracking the phase change of $\widetilde{u}(y)$ with streamwise distance (at each x the local phase value of $\widetilde{u}$ is taken at the wall-normal peak), the wavelength λ_{sls} ($= 2\pi/k_{sls}$) of the synthetic mode is estimated to be 15δ. The wave speed c of the synthetic mode is given by $c = f\lambda_{sls} = 0.59U_\infty$. The critical layer location y_c for the synthetic mode (i.e. the location in y_c where $\overline{U}(y) = c$) is estimated to be $y_c = 0.072\delta$ ($y_c^+ \approx 68$); this is marked by a dashed line in all relevant figures in this paper.

4. Modified phase relationships and small-scale organization

Skewness and amplitude modulation coefficient profiles are shown in figure 3(*b*) for canonical and forced flows at station-1. For the canonical flow, the behaviour of S and R with wall-normal distance y implies that large and small scales are close to being in phase ($S, R > 0$) near the wall, and gradually move towards being out of phase ($S, R < 0$) on approaching the layer edge; this trend is consistent with previous literature. In the presence of the synthetic large scale, the values of S and R are altered significantly, particularly in the wall-normal region where the synthetic mode is active (see the inset plot in figure 3*b*). There is a marked increase in the values of S and R in the region $0.02\delta < y < 0.1\delta$ and decrease in the region $0.1\delta < y < 0.4\delta$ in the presence of the synthetic large scale. The cross-over location $y/\delta = 0.1$ corresponds well to the synthetic mode peak location (see figure 3*c*), and is close to the estimated critical layer location. The results in figure 3(*b*) suggest that the synthetic large scale drives the envelope of all small scales towards being in and out of phase with it below and above its critical layer location respectively, thereby altering the natural large- and small-scale phase relationships (or the degree of amplitude modulation) in the flow.

A more direct influence of the synthetic large scale is seen on the small scales that couple triadically. Consider two small-scale triadic wavenumbers k_m, k_n ($> k_\gamma$) that couple directly to the synthetic large scale, i.e. $k_n - k_m = k_{sls}$. The envelope of k_m, k_n has a wavenumber of k_{sls} due to the triadic condition. Following an analysis similar to § 2, it can be shown that the square of the small-scale signal (u_S^2) phase-averaged with respect to the input forcing (denoted by $\widetilde{u_S^2} = \widetilde{\mathscr{E}}$) represents an amplitude-weighted average triadic envelope of all directly coupled small-scale wavenumbers k_m, k_n. In comparison with $\mathscr{E}$ (§ 2.2), $\widetilde{\mathscr{E}}$ denotes the triadic envelope of only those small scales that directly couple to the synthetic large scale, whereas $\mathscr{E}$ is the envelope

https://doi.org/10.1017/jfm.2015.79 Published online by Cambridge University Press

of all small scales. The phase relationship between $\widetilde{u}$ and $\widetilde{\mathscr{E}}$ can be quantified by a correlation coefficient (denoted by Ψ) between them, akin to the amplitude modulation coefficient defined by Mathis *et al.* (2009) for all large and small scales. The correlation coefficient Ψ is written as

$$\Psi = \frac{\langle \widetilde{u}\widetilde{\mathscr{E}} \rangle}{\langle (\widetilde{u})^2 \rangle^{1/2} \langle (\widetilde{\mathscr{E}})^2 \rangle^{1/2}}. \tag{4.1}$$

It should be noted that R gives the average phase between all large and small scales in the flow (including the synthetic scale when present), whereas Ψ is a measure of the phase between the synthetic scale and the average triadic envelope of small scales that are in direct coupling. Thus, Ψ represents the coupling due to one wavenumber within the broader u_L. The correlation coefficient $\Psi(y)$ at station-1 is shown in figure 3(*c*) along with the normalized energy of the synthetic large scale. The wall-normal locations where the synthetic large-scale energy drops to 15 % of its peak value are shown by dash-dot lines for reference; the region between these lines is where the effects of the synthetic large scale are expected to dominate. As the energy in the synthetic mode drops close to zero, the correlation coefficient Ψ becomes noisy (outside the 15 % energy reference lines). A clear organization in phase of directly coupled small scales by the synthetic large scale is seen in the region where the synthetic scale is active. The triadic small scales are in phase with the synthetic large scale ($\Psi = 1$) near the wall and out of phase ($\Psi = -1$) away from the wall; a sharp phase jump of π radians occurs at $y = 0.04\delta$, close to the estimated critical layer location. The phase behaviour of the directly coupled small scales is consistent with the altered large- and small-scale phase relationship suggested by the skewness and the amplitude modulation coefficient.

5. Conclusions

The analysis of skewness and the amplitude modulation coefficient presented here provides an alternate interpretation for both quantities in terms of phase; both are average measures of phase in triadic interactions between scales. By exciting a synthetic large-scale motion in a turbulent boundary layer, the natural (time-averaged) phase relationships in the flow as quantified by the skewness and the amplitude modulation coefficient can be modified in a quasi-deterministic manner. The influence of the synthetic large scale is strongly felt by small scales that are directly coupled in a triadic manner; a clear phase-locking or organization effect is seen. The experimental technique presented here helps us to better understand the scale coupling in turbulent wall-bounded flows through deterministic perturbations. In conjunction with the resolvent-based model of the Navier–Stokes equations (e.g. Sharma & McKeon 2013), the results presented here open the possibility of setting up a practical framework for favourable manipulation of energetic near-wall small-scale turbulence through large-scale inputs.

Acknowledgements

The authors gratefully acknowledge AFOSR (grant FA 9550-12-1-0469, program manager D. Smith) for the financial support of this work, and a graduate fellowship (S.D.) from the Resnick Institute at Caltech. We are grateful to K. Rosenberg for help with the wind tunnel set-up, and to R. Moarref and M. Luhar for many stimulating research discussions.

https://doi.org/10.1017/jfm.2015.79 Published online by Cambridge University Press

References

BANDYOPADHYAY, P. R. & HUSSAIN, A. K. M. F. 1984 The coupling between scales in shear flows. *Phys. Fluids* **27** (9), 2221–2228.

BROWN, G. L. & THOMAS, A. S. W. 1977 Large structure in a turbulent boundary layer. *Phys. Fluids* **20** (10), S243–S252.

CHUNG, D. & MCKEON, B. J. 2010 Large-eddy simulation of large-scale structures in long channel flow. *J. Fluid Mech.* **661**, 341–364.

DUVVURI, S. & MCKEON, B. J. 2014 Phase relationships in presence of a synthetic large-scale in a turbulent boundary layer. In *44th AIAA Fluid Dynamics Conference, Atlanta, GA, June 2014. AIAA Paper* 2014-2883.

HUSSAIN, A. K. M. F. & REYNOLDS, W. C. 1970 The mechanics of an organized wave in turbulent shear flow. *J. Fluid Mech.* **41**, 241–258.

HUTCHINS, N. & MARUSIC, I. 2007 Large-scale influences in near-wall turbulence. *Phil. Trans. R. Soc. Lond.* A **365**, 647–664.

JACOBI, I. & MCKEON, B. J. 2011 Dynamic roughness perturbation of a turbulent boundary layer. *J. Fluid Mech.* **688**, 258–296.

JACOBI, I. & MCKEON, B. J. 2013 Phase relationships between large and small scales in the turbulent boundary layer. *Exp. Fluids* **54**, 1481.

MARUSIC, I., MATHIS, R. & HUTCHINS, N. 2010 Predictive model for wall-bounded turbulent flow. *Science* **329**, 193–196.

MATHIS, R., HUTCHINS, N. & MARUSIC, I. 2009 Large-scale amplitude modulation of the small-scale structures in turbulent boundary layers. *J. Fluid Mech.* **628**, 311–337.

MATHIS, R., MARUSIC, I., HUTCHINS, N. & SREENIVASAN, K. R. 2011 The relationship between the velocity skewness and the amplitude modulation of the small scale by the large scale in turbulent boundary layers. *Phys. Fluids* **23**, 121702.

RAO, K. N., NARASIMHA, R. & NARAYANAN, M. A. B. 1971 The 'bursting' phenomenon in a turbulent boundary layer. *J. Fluid Mech.* **48**, 339–352.

SCHLATTER, P. & ÖRLU, R. 2010 Quantifying the interaction between large and small scales in wall-bounded turbulent flows: a note of caution. *Phys. Fluids* **22**, 051704.

SHARMA, A. S. & MCKEON, B. J. 2013 On coherent structure in wall turbulence. *J. Fluid Mech.* **728**, 196–238.

TALLURU, K. M., BAIDYA, R., HUTCHINS, N. & MARUSIC, I. 2014 Amplitude modulation of all three velocity components in turbulent boundary layers. *J. Fluid Mech.* **746**, R1.

https://doi.org/10.1017/jfm.2015.79 Published online by Cambridge University Press